MEMOIRS OF THE COLLEGE OF SCIENCE, UNIVERSITY OF KYOTO, SERIES B,
Vol. XXIX, No. 4 Geology and Mineralogy, Articl 1, 1962

The Relationships between the Petrology and the Radioactivity of Some Granitic Bodies (1)

By

Susumu NISHIMURA

Geological and Mineralogical Institute, University of Kyoto

(Received March 31, 1962)

Abstract

The distribution of radioactivity and chemical elements are traced in granitic intrusives. The results of determinations of racioactivity using a radioscope with a Lauritsen-element and a low-background counter show a tendency of the radioactive elements, *As* and *K* to concentrate towards the periphery of the batholith or stock. In general, the average radioactivity in batholiths is lower than in stocks. In intrusives, a core zone of lower than average radioactivity may be revealed if erosion has removed the roof and the upper part of the intrusions.

Introduction

The distribution of radioactive elements in granitic intrusions has been a subject of considerable interest.[1)2)3)] For example, studies of radioactive distribution in granitic intrusions have shown a tendency for radioactive elements to be concentrated towards the marginal part of the intrusion.

Studies of variations in distribution of radioactive and chemical elements across igneous contacts have yielded a great deal of information of granite.[4)] The purpose of the present study is to investigate the relationship between the abundance of radioactive elements and the petrology or mineralogy of granitic rocks.[5)]

The data presented in this paper consist of the radioactivity and the quantitative analyses of the chemical elements present in granitic rocks from three different plutons.

Part 1. The Distributions of Radioactivity and Chemical Elements in Granitic Bodies

Procedure

1. *Sampling*: Samples were collected from three granitic intrusions, Kitashirakawa, Tanakami-Mikumo and Rokkô. In order to obtain the possible average

value of radioactivity more than 2 *kg* of sample were collected at each site. These samples were pulverized to a 270 mesh sieve fineness and divided for the measurements.

2. *Semi-quantitative spectrographic analyses*: The procedure of the analyses adopted was the same as that used in the study of variation in chemical elements across igneous contacts previously reported.[4] The spectrograph is taken in the following conditions:

Spectral region	2400–4600 $\AA$ (Second order).
Slit width	20 μ.
Exposure period	30 *sec.*
Current	D.C. 15 *A.*

These conditions are good for general elements but rather unfavourable for *Th*, *U* and *K*.

3. *Measurement of alpha-radioactivity*: The measurement of alpha-radioactivity was made by means of a radioscope with a Lauritsen element.[4]

As the radioactive disintegration energy in rock is entirely converted into heat, the contribution of radioactive elements to heat generation in rock may be considered as nearly proportional to those of the ionization effects in air of the respective radio-elements. According to K. Rankama, the amount of heat generated by the alpha-radioactive elements in granite is as follows:

Radioactive family or nuclide	Calculated annual rate of heat generation by alpha-activity in granite 10^{-6} *cal/g.*
Uranium and Actinium families	3.00
Thorium family	2.74
Samarium	0.006

From this, it may be inferred that family-making radio-elements have overwhelmingly high alpha-radioactivity and its variation corresponds to variations in the amounts of uranium and thorium.

4. *Measurement of beta-radioactivity*: Measurement of beta-radioactivity was made with a low-background gas-flow counter (*LBC–1*).[4] Six sheets of *Al*–foil (9.6 mg/cm^2, in total) were used as an alpha-ray absorber.

The effect of absorption of beta-rays by *Al*–foil and by the sample itself is considered here. The absorption of alpha-rays has been studied by Z. Hatuda and J. Nagai,[6] and G. D. Finney and R. D. Evans.[7]

The half-value layer a of the beta-rays in the absorbing foil and source can be determined with good accuracy. The calibration is obtained from the relation

$$a = 0.046E^{3/2} \qquad \cdots\cdots(1)$$

where a is the half value layer in g/cm^2 and E is the maximum energy of beta-rays in *Mev*. Values for the half-value layer a of beta-radioactive elements are obtained as shown in Table 1.

Table 1. The half-value layer for natural beta-ray.

Radio-element	Coefficient of branches, (%)	Maximum energy, E, (*Mev*)	Half-value layer, *a*, (g/cm^2)	Number of beta-emissions in usual granite, ($\times 10^{-2} g^{-1}$)
Uranium family				
^{234}Th	100	0.193	0.0039	4.11
^{234}Pa	100	2.31	0.161	4.11
^{218}Po	0.04			
^{214}Pb	99.96	0.65	0.0241	4.11
^{218}At	0.0004			
^{214}Bi	99.96	3.17	0.260	4.11
^{210}Tl	0.04	1.80	0.111	0
^{210}Pb	100	0.023	0.000161	4.11
^{210}Bi	100	1.17	0.0580	4.11
^{206}Tl	5×10^{-5}			
Thorium family				
^{228}Ra	100	0.012	0.00006	5.37
^{228}Ac	100	0.218	0.00469	5.37
^{216}Po	0.013			
^{212}Pb	100	0.589	0.0102	5.37
^{212}Bi	66.3	2.25	0.155	3.56
^{208}Tl	33.7	1.79	0.110	1.81
Actinium family				
^{231}Th	100	0.302	0.0076	0.0168
^{227}Ac	98.8	0.0455	0.00045	0.0166
^{223}Fr	1.2	1.15	0.0566	0.0002
^{215}Po	5×10^{-4}			
^{211}Pb	100	1.39	0.0754	0.0168
^{211}Bi	0.32			
^{207}Tl	99.68	1.44	0.0796	0.0168
Single naturally radioactive nuclide				
^{40}K	0.0119	1.325	0.0704	72.3

For accurate quantitative determination of the number of beta-particles, corrections for sensitivity of the instrument, thickness of the source and absorber, and back scattering of the particles may be made as follows.

If N is the number of particles emitted per unit time,
f_B is the correction coefficient for back scattering,
f_A is the correction coefficient for absorption by *Al*-foils,
f_S is the correction coefficient for thickness of the source,
f_i is the correction coefficient for the sensitivity of the instrument,
and f_g is the correction coefficient for geometry.

The number of recorded particles n is expressed as

$$n = Nf_B f_A f_S f_i f_g \qquad \cdots\cdots(2)$$

In the present case, comparative measurements were used and therefore f_i and f_g are constants. The correction coefficient for back scattering f_B increases with increasing thickness d of the back material and theoretically reaches the maximum value at $d=0.5R$. In practice, however, the maximum value is attained at $d=0.2R$, R being the range of beta-particles. In this measurement the saturated value is used and may be considered constant at about 1.45.[8)]

Table 2. Calculated each coefficient and number of beta-emissions for average granite.*

Radio-element	f_A	f_S	$f_A \cdot f_S$	$N \cdot f_A \cdot f_S$ ($\times 10^{-2}$)
Uranium family				
^{234}Th	0.232	0.014	0.003	0.013
^{234}Pa	0.960	0.479	0.450	1.851
^{214}Pb	0.759	0.085	0.064	0.264
^{214}Bi	0.975	0.608	0.593	2.435
^{210}Tl	0.942	0.362	0.341	0.000
^{210}Pb	0.000	0.000	0.000	0.000
^{210}Bi	0.321	0.204	0.066	0.269
				total 4.833
Thorium family				
^{228}Ra	0.000	0.000	0.000	0.000
^{228}Ac	0.242	0.017	0.004	0.022
^{212}Pb	0.523	0.036	0.019	0.100
^{212}Bi	0.958	0.458	0.439	0.563
^{208}Tl	0.915	0.358	0.327	0.610
				total 2.295
Actinium family				
^{231}Th	0.417	0.027	0.011	0.0002
^{227}Ac	0.000	0.002	0.000	0.0000
^{223}Fr	0.889	0.199	0.177	0.0004
^{211}Pb	0.916	0.265	0.243	0.0041
^{207}Tl	0.920	0.280	0.258	0.0043
				total 0.0090
Single naturally radioactive nuclide				
^{40}K	0.910	0.248	0.225	16.30

* Evance and Goodman (1941).

Let the thickness of radioactive source and absorber be l and l_1, respectively, then the correction coefficients for absorption by the aluminium foils f_A and for the thickness of the radioactive source f_S are

$$f_A = \left(\frac{1}{2}\right)^{l_1/a} \qquad \cdots\cdots(3)$$

and

$$f_S = \frac{1}{l}\int_0^l \left(\frac{1}{2}\right)^{x/a} dx = \frac{1-\left(\frac{1}{2}\right)^{l/a}}{0.693\cdot\frac{l}{a}} \qquad \cdots\cdots(4).$$

In these experiments, l_1 is 9.6 mg/cm^2 and the thickness of sample l is 0.41 g/cm^2. Using these values, the coefficients f_A and f_S are obtained as given in the left half of Table 2.

If N_{UI} is the *beta-emissions/g/sec* of each uranium-family-element in equilibrium from average granite,

$$N_{UI} = 6.06\times10^{-23}\cdot F\cdot\lambda_{UI}\cdot\frac{UI}{W_{UI}} \qquad \cdots\cdots(5),$$

where F = the coefficient for branches of way of decay in percent,
λ_{UI} = a fraction of ^{238}U transformed per second,
UI = the amount of ^{238}U in the samples in g/g,
and W_{UI} = the atomic weight of ^{238}U.

On the other hand, the amount of radioactive elements in the average granite and the decay constants are:

Radioactive family	Contents in granite, * (ppm)	Decay constant, ** (sec^{-1})
Uranium family	3.0	4.86×10^{-18}
Actinium family	2.1×10^{-2}	3.11×10^{-17}
Thorium family	13	1.58×10^{-18}
Potassium (beta-decay nuclide)	310	1.54×10^{-17}

* Evans and Goodman (1941), ** Yagoda (1949).

Hence, for the each nuclei of uranium family in equilibrium,

$$N_{UI} = 4.11\times10^{-2}F \qquad \cdots\cdots(6).$$

Similarly, for each nuclei of the actinium and thorium families and potassium, the emissions of *beta-particles/g/sec* are

$$N_{AcU} = 1.68\times10^{-8}F,$$
$$N_{Th} = 5.37\times10^{-2}F,$$
and $$N_K = 7.37\times10^{-1}F.$$

From the number of emissions of beta-particles per second from each nucleous in 1 g of average (Table 1) and from the ratio of the emissions of beta-particles from each family (Table 2), we obtain:

$$n_{UI-F} : n_{Th-F} : n_{AcU-F} : n_K = 2.11 : 1 : 0.00 : 7.10$$

In summary, the variations of potassium content are largely reflected in those of beta-radioactivity, whilst the variations of uranium and thorium contents are mainly reflected in those of alpha-radioactivity.

Some descriptions on the geology of the localities from where samples were taken

1. *Kitashirakawa granite*: The Kitashirakawa granite is a biotite granite, occasionally associated with a small quantity of hornblende, and is penetrated by different dyke rocks. This granite intrudes into Paleozoic rocks which are often altered to hornfels by contact metamorphism. Distributions of alpha-activity along traverses across contact boundaries have been investigated.[4] From these results, the Kitashirakawa granite is classified into the second-type. The distribution of *Ra* content of this body also has been investigated by T. Asayama[9] and is shown in Fig. 4-1. It is seen that for 14 granites an increase in radioactivity is associated with increases in amounts of silica and potassium oxide.

2. *Tanakami-Mikumo granite*: The Tanakami granite is an intrusive body elliptical in shape. The Mikumo granite is a batholithic intrusion, making connexion with a former stock in its southwestern part. Tanakami granite is mainly coarse-grained, but sometimes medium- and fine-grained or porphyritic containing variable amounts of biotite. Mikumo granite is a coarse-grained hornblende biotite granite. The contact metamorphic rocks are hornfels for the Tanakami granite, schistose biotite hornfels for the Mikumo granite. Asayama's measurement[10] of radium content for these rocks are shown in Fig. 4-2. The radium content of 13 granites from Tanakami area ranges from 1.16×10^{-12} to 3.23×10^{-12} and averages $(2.04\pm0.12)\times10^{-12}$ *Ra g/g*, that of 11 granites from Mikumo area ranges from 0.43×10^{-12} to 1.34×10^{-12} and averages $(0.86\pm0.06)\times10^{-12}$ *Ra g/g*. Hence, marked differences in the ranges and the average of the radium content between these two groups of granites are observed. Separately, the amount of radium correlates with the amount of oxide in each of these two areas. The distribution of alpha-activity across contacts has been investigated, and the Tanakami stock is classified as the first type.[6]

3. *Rokkô granite*: The Rokkô mountain mass consists mainly of granite. These are biotite granite, hornblende granodiorite and hornblende-bearing biotite granite. The biotite granite may be divided into medium-grained, coarse-grained and fine-grained varieties. These granitic rocks intrude into Palaeozoic formations. Many kinds of dykes intruded into the granitic mass.

Results

The results of radioactivity determination are shown in Table 3 and in Figs. 1 to 3. Semi-quantitative spectrographical analyses listed in Table 4.

Table 3. Radioactivity of granitic rocks.

Locality	α-activity, (*div/min*)	β-activity, (*cpm*)
Kitashirakawa		
biotite granite (7)	0.45±0.02	10.1±0.6
porphyritic biotite granite (6)	0.66±0.03	10.7±0.4
Tanakami (6)	1.01±0.05	10.4±0.4
Mikumo (9)	0.72±0.09	13.3±1.2
Rokkô		
coarse-grained biotite granite (16)	0.87±0.05	13.2±0.3
medium-grained biotite granite (5)	0.71±0.03	12.7±0.5
fine-grained biotite granite (3)	0.49−0.02	10.4±0.1
liparite (1)	0.45	7.6
granite porphyry (1)	0.80	9.8

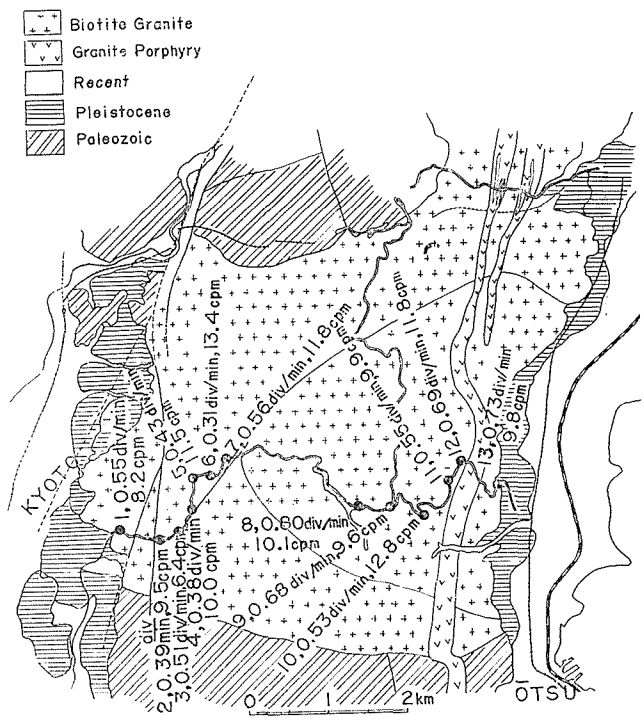

Fig. 1. Distribution of radioactivity (Kitashirakawa).

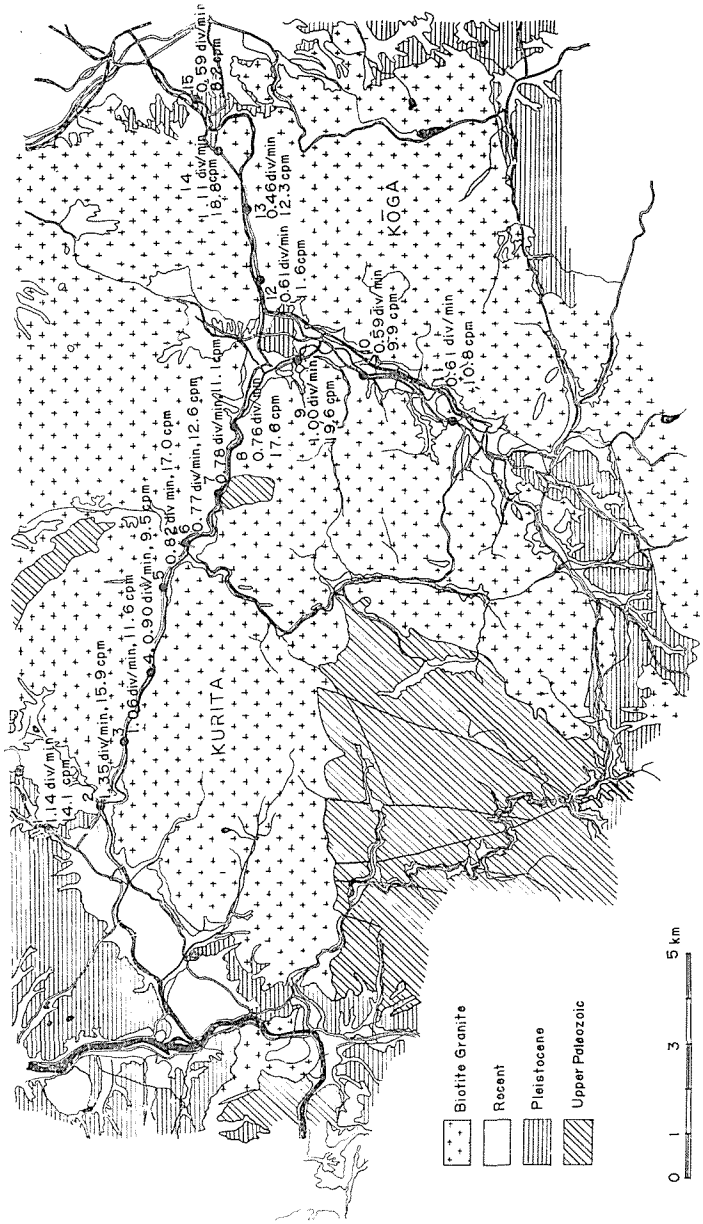

Fig. 2. Distribution of radioactivity (Tanakami-Mikumo).

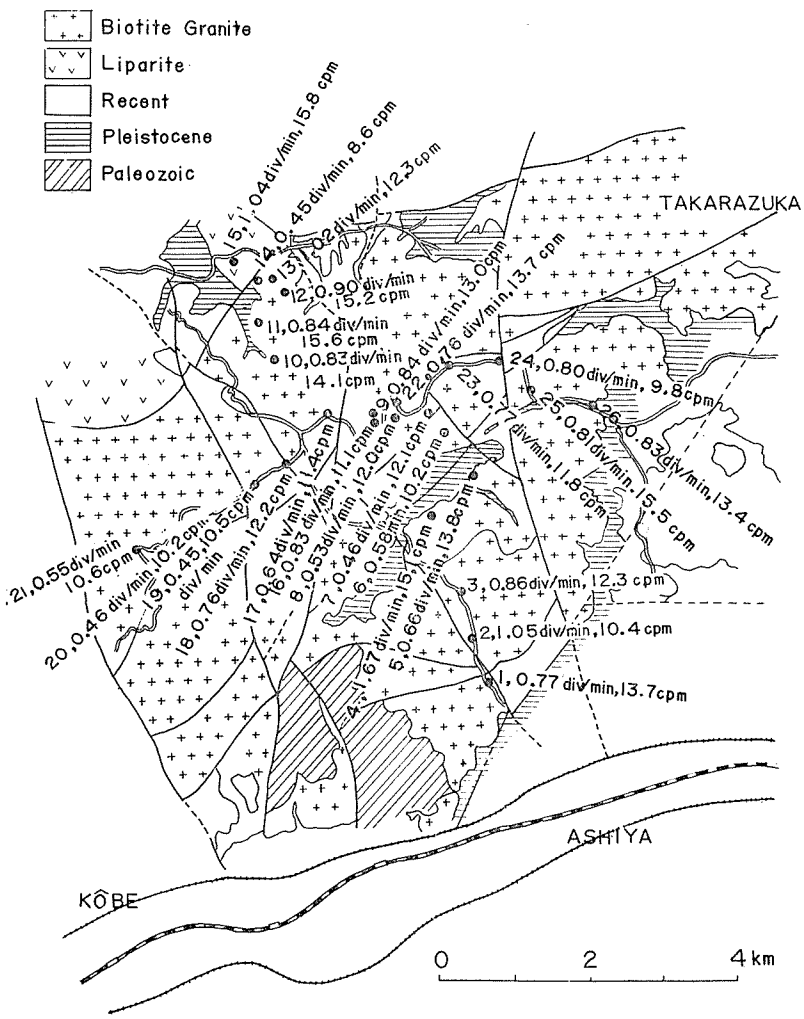

Fig. 3. Distribution of radioactivity (Rokkô).

Table 4. Quantitative variations of the amounts of chemical elements in granite of each locality.

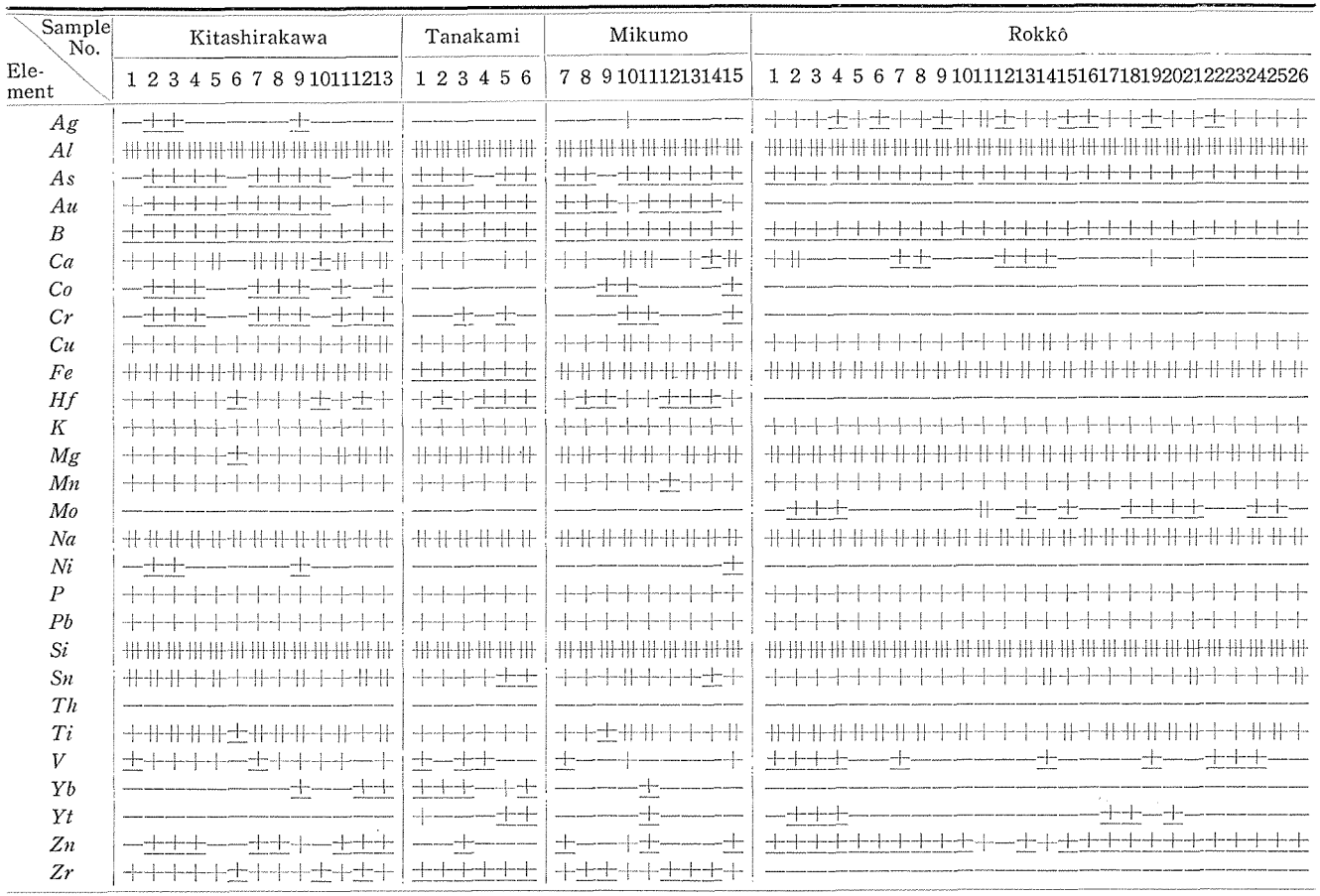

strong, *moderate*, *weak*, *weak*, *weak*, t *trace*, — *undetectable*.

The frequency of radioactivity of samples from each locality is given in Table 5. From these results, Tanakami granites is proved to be the highest in radioactivity.

Table 5-1. The frequency of α-activity in granite of each locality.

α-activity (div/min) / Locality	0.26～0.50	0.51～0.75	0.76～1.00	1.01～1.25	1.26～1.50	1.51～1.75
Kitashirakawa	4	8	1			
Tanakami-Mikumo	1	4	6	3	1	
Tanakami			3	2	1	
Mikumo	1	4	3	1		
Rokkô	4	5	13	3		1
Biotite granite	3	5	12	3		1
coarse-grained	1	2	9	3		1
medium-grained		2	3			
fine-grained	2	1				
Liparite	1					
Granite Porphyry			1			

Table 5-2. The frequency of β-activity in granite of each locality.

β-activity (cpm) / Locality	5.1～7.5	7.6～10.0	10.1～12.5	12.6～15.0	15.1～17.5	17.6～
Kitashirakawa	1	6	4	2		
Tanakami-Mikumo		3	5	2	2	3
Tanakami		1	1	2	2	
Mikumo		2	4			3
Rokkô		2	13	6	5	
Biotite Granite			13	6	5	
coarse-grained			8	3	5	
medium-grained			2	3		
fine-grained			3			
Liparite		1				
Granite Porphyry		1				

Table 6 gives the average quantities and Table 7 the variations for each element in Kitashirakawa, Tanakami-Mikumo and Rokkô intrusives. From the spectrographical analyses, the quantitative variations of *Ag*, *As*, *Au*, *Ca*, *Co*, *Cr* and *Cu* are remarkable for the Kitashirakawa and Tanakami-Mikumo areas,

Table 6. The average quantities of each element in granite of each locality.

Element \ Locality	Kitashirakawa	Tanakami-Mikumo			Rokkô					
		Average	Tanakami	Mikumo	Average	coarse g.b.g.	medium g.b.g.	fine g.b.g.	Li-paule	G. Porph.
Ag	t	t	—	t	+	+	+	+	+	+
Al	##	##	##	##	##	##	##	##	##	##
As	±	±	±	±	±	±	±	±	±	±
Au	±	±	±	±	—	—	—	—	—	—
B	±	±	±	±	±	±	±	±	±	±
Ca	+	+	+	+	t	t	t	t	—	±
Co	±	t	—	t	—	—	—	—	—	—
Cr	±	±	t	t	—	—	—	—	—	—
Cu	+	+	+	+	+	+	+	+	#	+
Fe	#	#	#	#	#	#	#	#	#	#
Hf	+	±	±	±	—	—	—	—	—	—
K	+	+	+	+	+	+	+	+	+	+
Mg	+	#	#	#	#	#	#	#	#	#
Mn	+	+	+	+	+	+	+	+	+	+
Mo	—	—	—	—	±	±	t	±	±	—
Ma	#	#	#	#	#	#	#	#	#	#
Ni	t	t	—	t	—	—	—	—	—	—
P	+	+	+	+	+	+	+	+	+	±
Pb	+	+	+	+	+	+	+	+	+	+
Si	##	##	##	##	##	##	##	##	##	##
Sn	#	+	+	+	+	+	+	+	+	#
Th	—	—	—	—	—	—	—	—	—	—
Ti	+	+	+	+	#	#	#	#	+	#
V	+	±	±	±	t	t	t	t	±	±
Yb	t	t	±	t	—	—	—	—	—	—
Yt	—	t	±	t	t	t	t	t	—	—
Zn	±	t	t	±	±	±	±	±	±	+
Zr	+	±	±	±	—	—	—	—	—	—

Table 7. The variation of chemical elements in granite of each locality.

Element \ Lacality	Kitashira kawa	Tanakami-Mikumo			Rokkô			
		Average	Tanakami	Mikumo	Average	c.g.b.g.	m.g.b.g.	f.g.b.g.
Ag	—~±		—~+	—~+	±~#	±~#	±~+	±~+
Al		#~##	#~##	#~##				
As	—~±	—~±	—~±	—~±				
Au	—~+		±~+	±~+				
Ca	+~#	—~+	—~#	—~#	—~#	—~#	—~+	—~+
Co	—~±	—~±	—~±					
Cr	—~±	—~±	—~±	—~±				
Cu	+~#	+~#		+~#				
Hf	±~+	±~+	±~+	±~+				
Mg	±~#	+~#		+~#				
Mn		±~+		±~+				
Mo					—~#	—~#	—~±	
Ni	—~±	—~±		—~±				
Sn	+~#	±~#	±~+	±~#	+~#	+~#		+~#
Ti	±~#	+~#		+~#	+~#	+~#	+~#	
V	—~+	—~+	—~±	—~+	—~±	—~±	—~±	—~±
Yb	—~±	—~+	—~+	—~±				
Yt		—~+	—~+	—~±	—~+	—~±	—~+	—~±
Zn	—~+	—~+	—~±	—~+				
Zr	±~+		±~+	±~+				

and rather vague for the Rokkô granite. Rokkô granite samples are richest in *Ag* and *Mo*, and poorest in *Au*, *Ca*, *Co*, *Cr*, *Hf*, *Ni*, *V*, *Yb* and *Zr* as compared with the other two intrusions.

The distributions of alpha-radioactivity and beta-radioactivity (S. Nishimura) and radium and K_2O contents determined (T. Asayama[10]) are given in Figs. 4-1 to 4-3. In these figures, there is a tendency for an increase of alpha-radioactivity towards the outer margin of the batholiths, consideration being given to the effect of size variation of the major mineral constituents. In the Tanakami-Mikumo and Rokkô granites, there is a similer tendency in the quantitative variations of alpha- and beta-radioactivities.

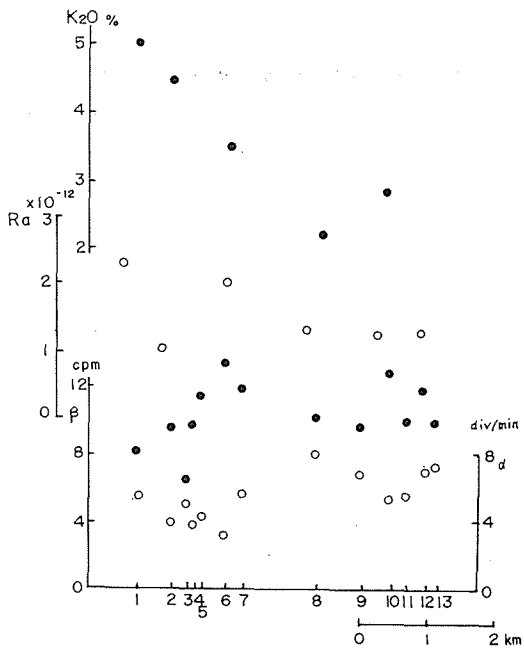

Fig. 4-1. Plot of the alpha-radioactivity (◦), beta-radioactivity (·), Ra content (◦) and K_2O content (·) across Kitashirakawa intrusive mass.

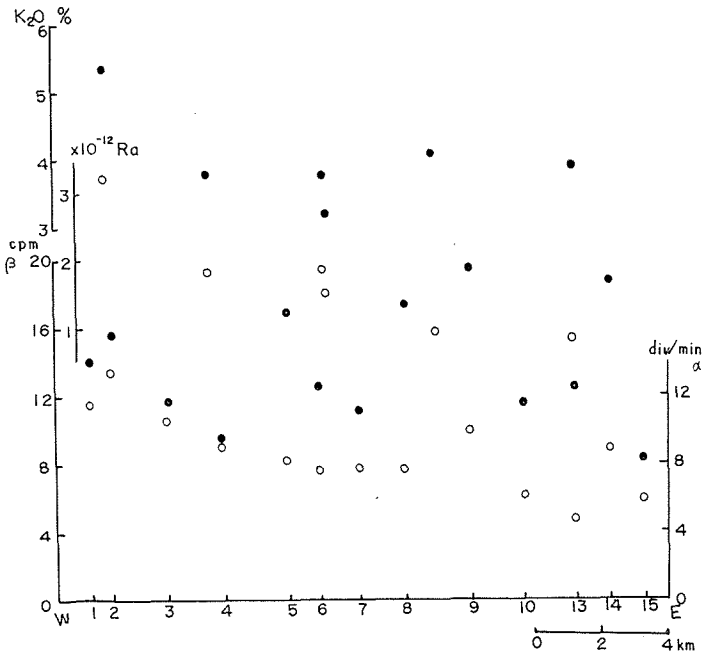

Fig. 4-2. Plot of the alpha-radioactivity (○), beta-radioactivity (·), Ra content (○) and K_2O content (·) across Tanakami-Mikumo intrusive mass.

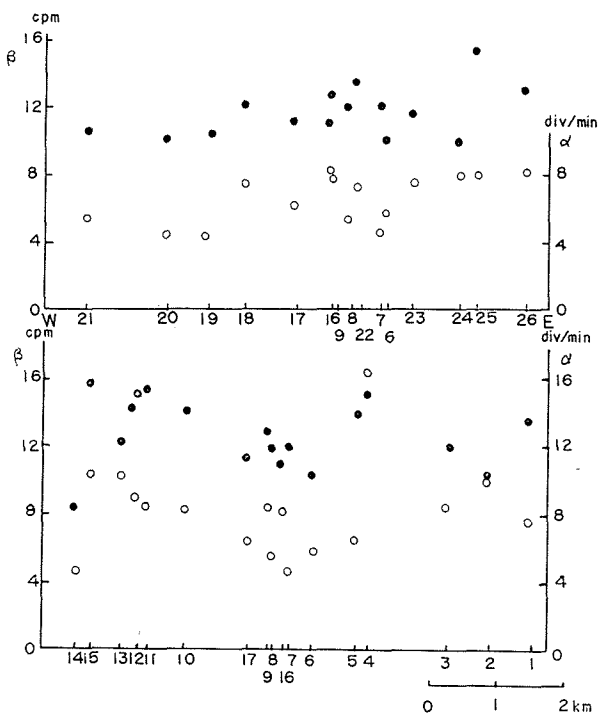

Fig. 4-3. Plot of the alpha-radioactivity (○) and beta-radioactivity (·) across Rokkō intrusive mass.

Discussion

(1) *Relationship between the quantitative variations of radioactivity and amounts of Ra and K_2O*: The distributions of radioactivity and amounts of *Ra* and K_2O in Kitashirakawa and Tanakami-Mikumo intrusions are given in Fig. 4. Radioactivity, and amounts of *Ra* and K_2O are seen to increase towards the margin of the intrusions. In the Tanakami-Mikumo intrusion, a marked difference in the range and average alpha-radioactivity and amount of *Ra* between these two granites are clearly observed but are vague for beta-radioactivity. This suggests a tendency for higher alpha-radioactivity and beta-radioactivity for later stage of granitic magma.

(2) *Relation between alpha- and beta-radioactivities*: The relation between alpha- and beta-radioactivities is shown in Fig. 5. In the Kitashirakawa granite, there is little relation of alpha-radioactivity to beta-radioactivity; in the Rokkō and Tanakami-Mikumo granite intrusions, alpha-radioactivity increases with increasing beta-radioactivity, but the trend is rather vague.

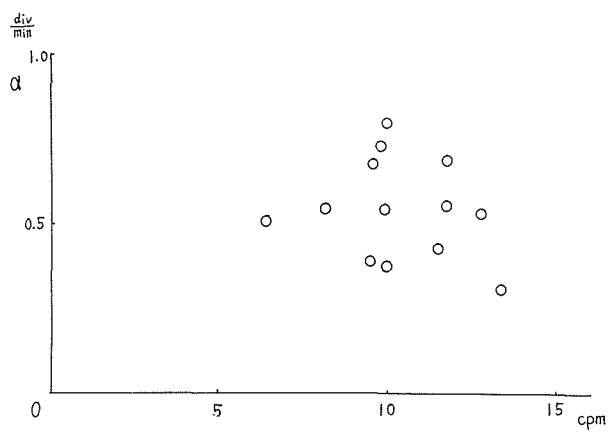

Fig. 5–1. Relation between alpha-radioactivity and beta-radioactivity (Kitashirakawa).

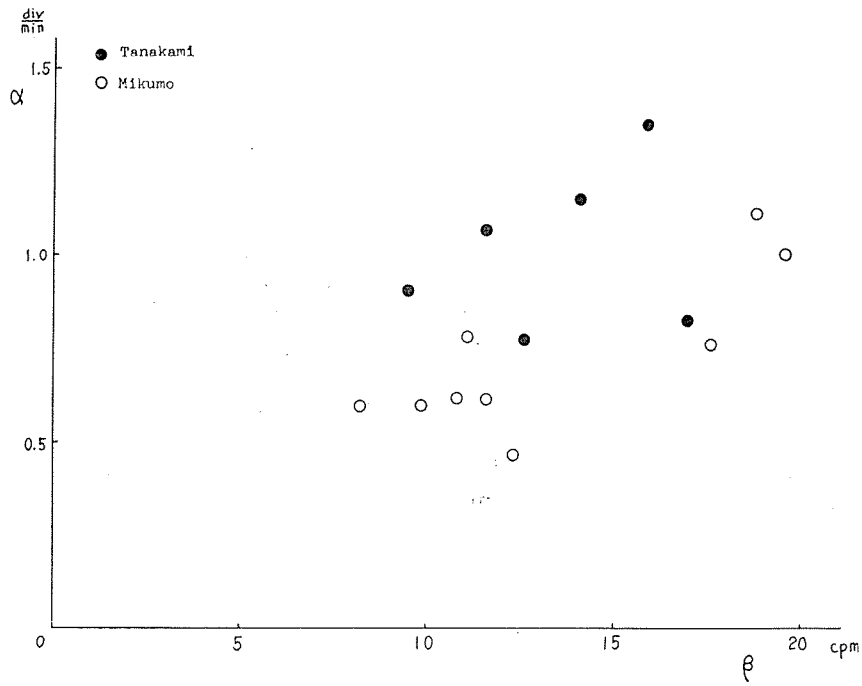

Fig. 5-2. Relation between alpha-radioactivity and beta-radioactivity (Tanakami-Mikumo).

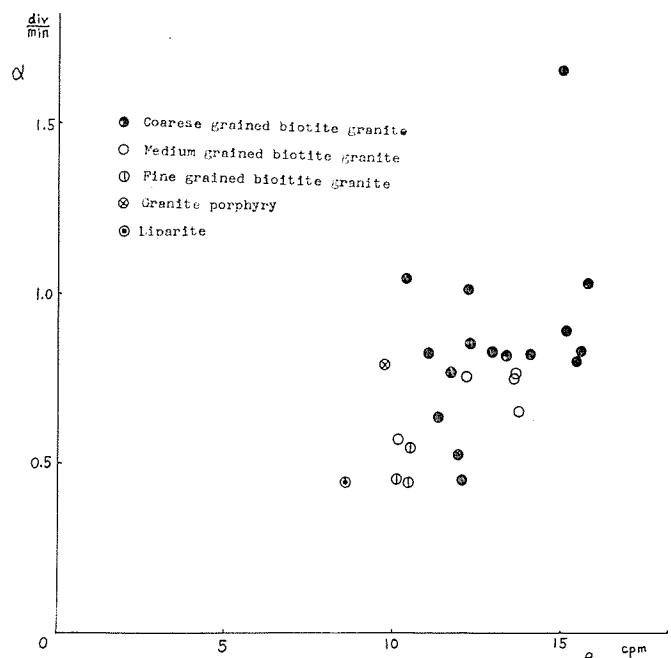

Fig. 5-3. Relation between alpha-radioactivity and beta-radioactivity (Rokkô).

(3) *Relation between radioactivity and quantitative variations of chemical elments*: Table 8 shows the relationship between radioactivity and the variations of the chemical elements, in each locality, and summarized results are shown as follows:

Locality	Increasing material			
	with increasing α-activity	with decreasing α-activity	with increasing β-activity	with decreasing β-activity
Kitashirakawa	*Ca*	*Ag, Ni, Sn*	*Ca, Co, Cr, V, (K)*	*Ag, Ni, Sn*
Tanakami	*Ca, As*	*Sn, Yb, Yt*	*As, (K)*	*Sn, Yb, Yt*
Mikumo		*Ag, Au, Ca, Co, Cr, Hf, Ni, Sn, Zr, V*	*(K)*	*Ca, Ag, Au, Co, Cr, Hf, Ni, Sn, Zr, V, Cu*
Rokkô	*V, Yt*	*Ag, Ca, Ti*	*(K)*	*Ag, Ca, Ti*
Average	*V*	*Hf, Ag, Ca, Co, Ni, Zr*	*(K)*	*Au, Mo, Sn, Ag, Ca, Co, Ni, Zr*

Table 8-1. The relation between radioactivity and semi-quantitative variations of chemical elements. (Kitashirakawa).

Element	α-radioactivity (div/min)			β-radioactivity (cpm)			
	0.26~0.50	0.51~0.75	0.76~1.00	5.1~7.5	7.6~10.0	10.1~12.5	12.6~15.0
Ag	t	t	—	±	t	—	—
Al	###	###	###	###	###	###	###
As	±	±	±	±	±	±	±
Au	±	±	±	±	±	±	±
B	±	±	±	±	±	±	±
Ca	±	±	##	±	##	##	±
Co	±	±	±	±	±	±	—
Cr	±	±	±	±	±	±	—
Cu	±	±	±	±	±	±	±
Fe	##	##	##	##	##	##	##
Hf	±	±	±	±	±	±	±
K	±	±	±	±	±	±	±
Mg	±	±	±	±	±	±	±
Mn	±	±	±	±	±	±	±
Mo	—	—	—	—	—	—	—
Na	##	##	##	##	##	##	##
Ni	±	t	—	±	t	—	±
P	±	±	±	±	±	±	±
Pb	±	±	±	±	±	±	±
Si	###	###	###	###	###	###	###
Sn	##	##	±	##	##	##	±
Th	—	—	—	—	—	—	—
Ti	##	##	##	##	##	##	##
V	±	±	±	±	±	±	±
Yb	—	t	—	—	t	t	—
Yt	—	—	—	—	—	—	—
Zn	±	±	±	±	±	±	—
Zr	±	±	±	±	±	±	±

Table 8-2. The relation between radioactivity and semi-quantitative

Element	Tanakami-Mikumo					Tanakami			Mikumo			
	α-radioactivity (div/min)											
	0.26 ~0.50	0.51 ~0.75	0.76 ~1.00	1.01 ~1.25	1.26 ~1.50	0.76 ~1.01	01.0 ~1.25	1.26 ~1.50	0.26 ~0.50	0.51 ~0.75	0.76 ~1.00	1.01 ~1.25
Ag	—	±	—	—	—	—	—	—	—	±	—	—
Al	###	###	###	###	###	###	###	###	###	###	###	###
As	±	±	±	±	±	±	±	±	±	±	±	±
Au	±	±	±	±	±	±	±	±	±	±	±	±
B	±	±	±	±	±	±	±	±	±	±	±	±
Ca	±	±	±	±	±	±	±	±	±	±	±	±
Co	—	±	t	—	—	—	—	—	—	±	t	—
Cr	—	±	t	t	—	t	±	—	—	±	—	—
Cu	±	±	±	±	±	±	±	±	±	±	±	±
Fe	##	##	##	##	##	##	##	##	##	##	##	##
Hf	±	±	±	±	±	±	±	±	±	±	±	±
K	±	±	±	±	±	±	±	±	±	±	±	±
Mg	##	±	##	##	##	##	##	##	##	±	##	##
Mn	±	±	±	±	±	±	±	±	±	±	±	±
Mo	—	—	—	—	—	—	—	—	—	—	—	—
Na	##	##	##	##	##	##	##	##	##	##	##	##
Ni	—	t	—	—	—	—	—	—	—	t	—	—
P	±	±	±	±	±	±	±	±	±	±	±	±
Pb	±	±	±	±	±	±	±	±	±	±	±	±
Si	###	###	###	###	###	###	###	###	###	###	###	###
Sn	±	±	±	±	±	±	±	±	±	±	±	±
Th	—	—	—	—	—	—	—	—	—	—	—	—
Ti	±	##	±	±	±	±	±	±	±	##	±	±
V	—	±	t	±	—	t	±	—	—	±	t	—
Yb	—	t	±	±	±	±	±	±	—	t	—	—
Yt	—	t	t	±	—	±	±	—	—	t	—	—
Zn	—	±	t	t	—	—	±	—	—	±	t	—
Zr	±	±	±	±	±	±	±	±	±	±	±	±

Table 8-3. The relation between radioactivity and semi-quantitative

Element	Biotite granite					Coarse-grained b.g.					Medium-grained b.g.	
	α-radioactivity (div/min)											
	0.26 ~0.50	0.51 ~0.75	0.76 ~1.00	1.01 ~1.25	1.51 ~1.75	0.26 ~0.50	0.51 ~0.75	0.76 ~1.00	1.01 ~1.25	1.51 ~1.75	0.51 ~0.75	0.76 ~1.00
Ag	±	±	±	±	±	±	±	±	±	±	±	±
Al	###	###	###	###	###	###	###	###	###	###	###	###
As	±	±	±	±	±	±	±	±	±	±	±	±
Au	—	—	—	—	—	—	—	—	—	—	—	—
B	±	±	±	±	±	±	±	±	±	±	±	±
Ca	±	±	t	±	—	±	±	t	±	—	—	±
Co	—	—	—	—	—	—	—	—	—	—	—	—
Cr	—	—	—	—	—	—	—	—	—	—	—	—
Cu	±	±	±	±	±	±	±	±	±	±	±	±
Fe	##	##	##	##	##	##	##	##	##	##	##	##
Hf	—	—	±	—	—	—	—	—	—	—	—	—
K	±	±	±	±	±	±	±	±	±	±	±	±
Mg	##	##	##	##	##	##	##	##	##	##	##	##
Mn	±	±	±	±	±	±	±	±	±	±	±	±
Mo	±	t	±	±	±	—	—	±	±	±	—	t
Na	##	##	##	##	##	##	##	##	##	##	##	##
Ni	—	—	—	—	—	—	—	—	—	—	—	—
P	±	±	±	±	±	±	±	±	±	±	±	±
Pb	±	±	±	±	±	±	±	±	±	±	±	±
Si	###	###	###	###	###	###	###	###	###	###	###	###
Sn	±	±	±	±	±	±	±	±	±	±	±	±
Th	—	—	—	—	—	—	—	—	—	—	—	—
Ti	±	±	±	##	##	##	##	±	##	##	##	##
V	±	—	t	t	±	±	—	t	t	±	—	±
Yb	—	—	—	—	—	—	—	—	—	—	—	—
Yt	t	t	t	t	±	—	±	t	t	±	—	t
Zn	±	±	±	±	±	±	±	±	±	±	±	±
Zr	—	—	—	—	—	—	—	—	—	—	—	—

variations of chemical elements (Tanakami-Mikumo).

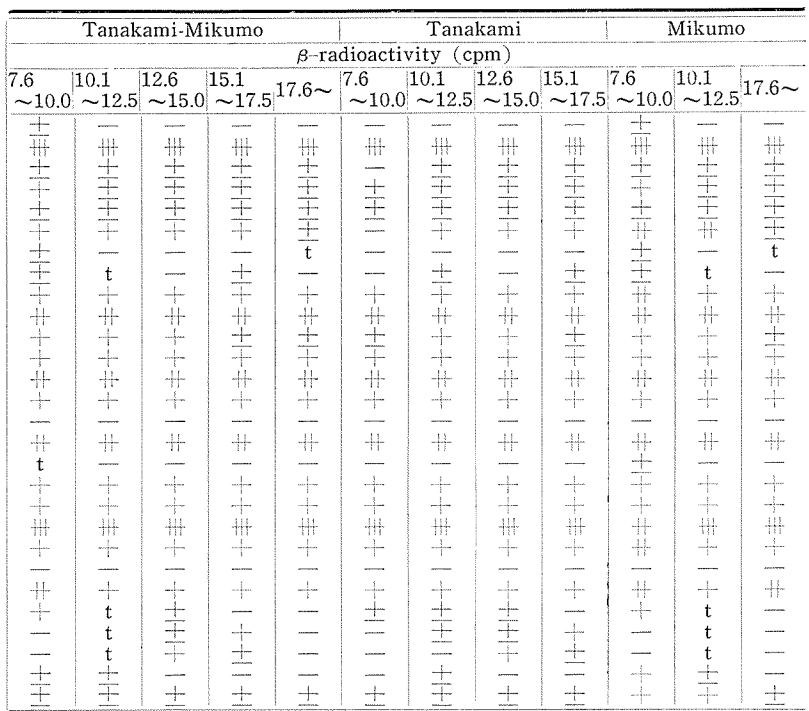

variations of chemical elements (Rokkô).

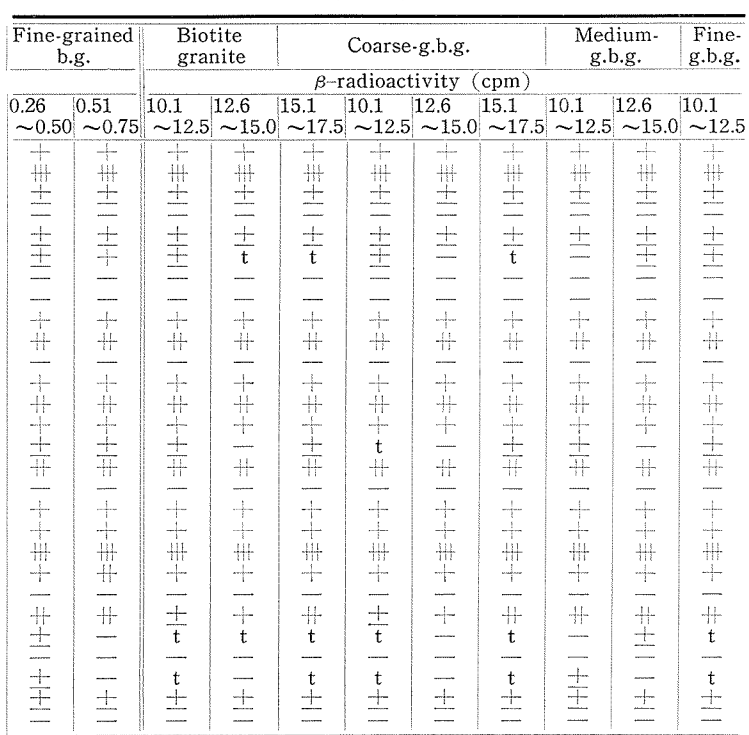

In summary, the relationship between radioactivity and variations of chemical elements over the whole intrusion are shown in Table 8-4. The general trends show a marked increase of alpha-radioactivity with decreasing *Hf*: of beta-radioactivity with decreasing *Au*, *Mo*, and *Sn*, and an increase of both radioactivities with decreasing *Ag*, *Ca*, *Co*, *Ni* and *Zr*. Alpha-radioactivity increases with increasing *V*.

Conclusions

From the above results, following conclusions may be deduced; (1) concentration of alpha- and beta-radioactivities towards the outer margins of the batholiths, (2) remarkable variations in quantities of *Ag*, *As*, *Au*, *Ca*, *Cr* and *Cu* in the Tanakami-Mikumo and Kitashirakawa intrusions, (3) an increase of both radioactivities with increasing grain-size of the major minerals present in the rocks and (4) the average values of both radioactivities in stocks are higher than those in batholiths.

The general trends of the relation between ratioactivity and variations of chemical elements indicate that an increase of alpha-radioactivity is accompanied with a decrease of *Hf*. Beta-radioactivity increases with decreasing *Au*, *Mo* and *Sn*. The increase of both radioactivities with decreasing *Ag*, *Ca*, *Co*, *Cr*, *Ni* and *Zr*. Alpha-radioactivity increases with increasing *V*.

Part 2. The Distributions of Radioactivity and Mode of Minerals in Granitic Bodies

Petrographical modal analyses were made with unoriented thin sections on the same samples used for spectrographic analyses and measurements of radioactivity. Modal analyses of most of the individual samples are given in the following paragraph.

(1) *The mineral contents obtained by modal analyses of various types of granitic rocks and the variation of the mineral contents within individual intrusions*:

Table 9 shows that the differences of mineral contents for various granitic rocks are smaller than the differences with individual intrusions; for examples, in Kitashirakawa granite the amount of quartz ranges from 26.6% to 55.2%, but the average of that of various different types of granitic rocks ranges from only 38.3% to 32.7%.

The differences in mineral assemblage and radioactivity of the Kitashirakawa granite intrusion shows the western part to be different from the eastern part. The western part is abundant in quartz, but poor in potash-feldspar and mica. The eastern part is abundant in potash-feldspar, but poor in quarts. Both radioactivities of granite samples from the western part is higher than those from the eastern part.

The Tanakami granite has uniform mineral assemblage, but the Mikumo

Table 9. Modal analyses of granitic rocks.

Specimen	R.	C.I.	Quartz	Plagioclase	Potash-feldspar	Mica	Hornblende	Opaques	Zircon	Apatite	Sphene	Epidote	Chlorite
Kitashirakawa													
1	2.05	12.9	29.0	19.5 (olig.)	40.0	10.2	tr$^+$	0.5	tr$^+$		0.2	0.2	0.3
2	2.33	14.4	29.2	17.5 (olig.)	40.7	11.1	tr$^+$	0.3	tr$^+$	0.1	0.5		0.6
3	2.80	12.9	26.6	16.3 (olig.)	45.7	10.1	tr$^+$	0.5	tr$^+$	0.2	tr		0.6
8	2.48	15.5	26.7	17.2 (Lab.)	42.7	12.5		0.6	tr$^+$				0.3
10	1.98	7.8	55.2	12.6 (Lab.)	25.0	5.5		1.7	tr				tr
12	0.98	4.2	54.8	20.8 (And.)	20.4	3.2		0.8	tr				tr
13	1.27	6.1	46.7	20.9 (And.)	26.6	5.2		0.5	tr				tr
Tanakami													
1	1.29	9.2	35.4	24.5 (Lab.)	31.7	7.9		0.1	tr$^+$				0.4
2	1.62	5.4	30.1	24.7 (Lab.)	40.0	4.4		0.1	0.3				0.3
3	2.14	7.3	32.3	19.4 (Lab.)	41.5	6.3		0.1	tr$^+$				0.4
4	2.79	11.2	38.8	13.5 (Lab.)	37.7	6.3		1.1	tr$^+$				2.7
5	2.91	35.0	26.8	12.1 (Lab.)	35.2	10.2	10.0	2.1	tr$^-$		tr		3.6
Mikumo													
6	2.15	6.7	26.0	21.5 (And.)	46.2	1.2	2.4	6.6	tr				1.1
7	2.77	4.0	39.7	15.0 (And.)	41.5	0.6	0.7	1.1	tr$^-$				1.4
8	2.88	4.3	44.7	10.3 (And.)	40.9	0.7	1.2	1.1	tr$^-$				1.1
9	5.76	2.0	56.1	6.2 (And.)	35.7	0.8	1.1	0.1	tr$^-$				tr$^-$
10	3.49	2.9	33.6	14.2 (And.)	49.5	0.2	1.0	0.3	tr$^-$				1.3
11	3.36	5.9	29.8	14.8 (And.)	49.8	1.2	4.0	0.2	tr$^+$				0.2
12	3.64	3.8	40.0	12.1 (And.)	44.1	1.0	2.0	0.2	tr$^-$				0.5
13	3.70	8.0	32.0	12.9 (And.)	47.7	2.0	3.5	0.9	tr				1.0
14	10.22	7.4	32.5	5.4 (And.)	55.2	0.4	4.0	0.5	tr$^+$				1.0
Rokkô													
1	1.66	4.1	37.8	21.9 (And.)	36.4	2.5		1.2					0.2
2	2.52	2.5	45.1	14.9 (And.)	37.6	1.5		0.9	tr				tr$^+$
3	1.79	5.5	26.4	24.5 (And.)	43.9	4.1		1.1	tr				tr$^-$
4	0.81	3.5	48.3	26.9 (And.)	21.4	1.1		1.8					0.5
6	1.16	3.0	33.2	29.6 (And.)	34.3	1.4		0.9	tr				0.6
7	0.83	5.5	44.8	27.3 (And.)	22.7	3.6		1.2	tr				0.4
8	3.01	2.0	47.9	12.5 (And.)	37.6	1.6		0.2					0.2
9	1.29	2.0	45.8	22.8 (And.)	29.5	1.4		0.4					0.2
10	1.77	12.7	34.9	19.4 (And.)	34.4	8.8		2.2	tr				0.3
11	1.78	12.1	32.8	20.3 (And.)	36.1	8.2		2.3	tr				0.3
12	2.00	4.0	39.5	18.9 (And.)	37.8	2.8		1.0	tr				tr$^-$
13	2.11	1.6	29.5	22.1 (And.)	46.6	1.0		0.6					tr$^-$
15	1.19	2.2	43.3	24.9 (And.)	29.6	0.3		1.9					tr$^-$
16	1.07	4.3	46.7	23.8 (And.)	25.4	3.3		0.8					tr$^-$
17	1.74	2.2	47.2	18.4 (And.)	32.1	1.6		0.6					tr$^-$
19	2.34	1.0	37.7	18.4 (And.)	43.0	0.6		0.3					0.1
21	2.09	5.0	35.6	19.6 (And.)	40.0	2.9		1.9	tr				tr$^-$
22	1.37	1.6	31.7	28.1 (And.)	38.6	1.2		0.4	tr				tr$^-$
23	2.83	2.1	40.5	15.0 (And.)	42.5	2.0		0.1	tr				tr$^-$
24	1.66	3.1	46.2	19.1 (And.)	31.8	2.5		0.5	tr				tr$^-$
25	1.48	6.3	30.2	25.8 (And.)	38.1	4.7		1.2	tr				tr$^-$
26	2.09	1.7	28.1	22.7 (And.)	47.4	1.5		0.4	tr				tr$^-$

R. is potash-feldspar/plagioclase ratio.
C.I. is colour index; muscovite counted as a dark mineral.
tr$^-$ is a very scarce trace mineral.
tr$^+$ is abundant trace mineral.
All values of percentages are reported to not more than two significant figures.

granite is variable. The latter is more abundant in potash-feldspar than the former and has lower alpha-radioactivity. The beta-radioactivity of the latter is higher than that of the former.

Rokkô granites are divided into biotite-granite, hornblende granodiorite and hornblende bearing biotite granite.[11]

(2) *The relationships between radioactivity and various petrographic parameters*:

Potash-feldspar/plagioclase ratio (hereafter denoted by R), quartz content and colour index (defined by Shand, 1947) have all been considered as indices of general petrogenetic evolution of granitic rocks. These petrographic parameters have been plotted against alpha- and beta-radioactivities and beta-radioactivity/alpha-radioactivity ratio (β/α) in order to give further evidence concerning the behaviour of radioactive elements during igneous petrogeneses. Figs. 6 to 9 show the relationships.

Scatter diagrams of R vs. alpha- and beta-radioactivity and β/α ratio are shown in Figs. 6-1 to 6-3. Both beta-radioactivity and β/α ratio show little if any relationships to R; but both may increase slightly with increasing R, the points being very scattered for each locality. According to J. W. Whitefield, J. J. W. Rogers and J. A. S. Adams[12] relationships between *Th* and *U*, and R follow two trends; first, *Th* increases more rapidly with increasing R than *U* does, and secondly, alpha-radioactivity increases with increasing R.

Relationships between alpha- and beta-radioactivities and β/α ratio and colour index are shown in Figs. 7-1 to 7-3. Alpha- and beta-radioactivities are

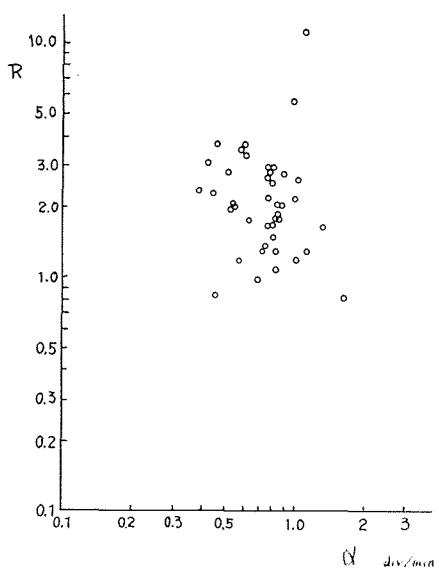

Fig. 6-1. Scatter diagram of R vs. alpha-radioactivity.

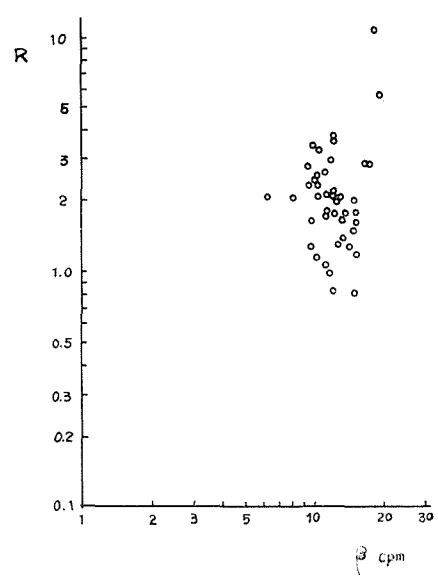

Fig. 6-2. Scatter diagram of R vs. beta-radioactivity.

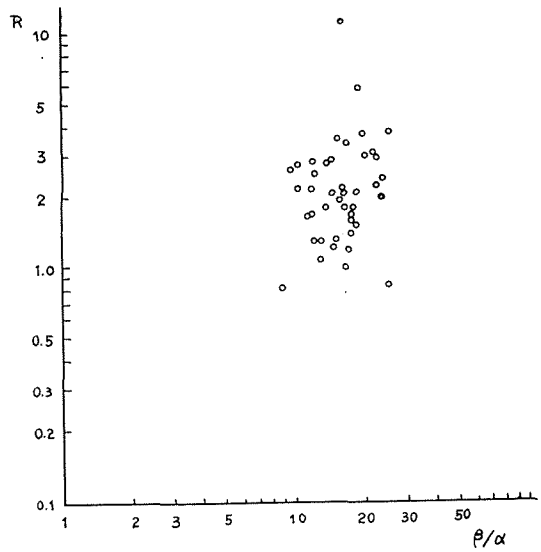

Fig. 6-3. Scatter diagram of R vs. β/α ratio.

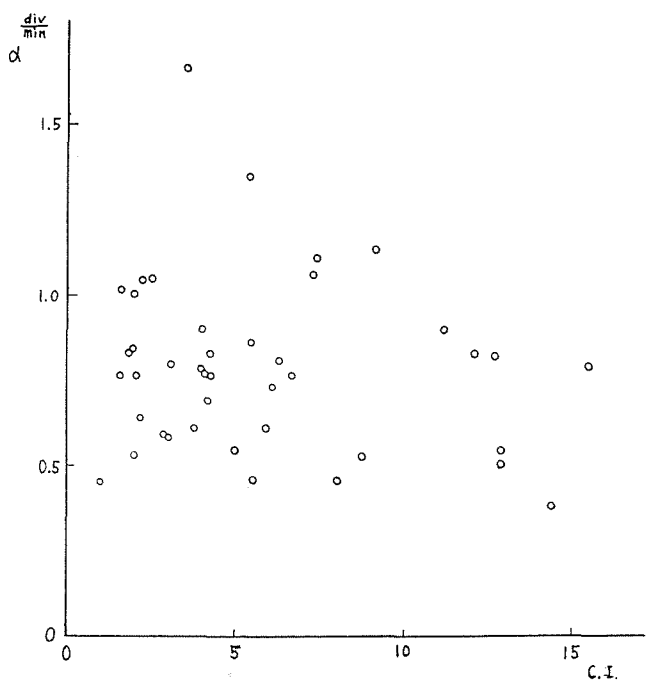

Fig. 7-1. Relationship between alpha-radioactivity and colour index.

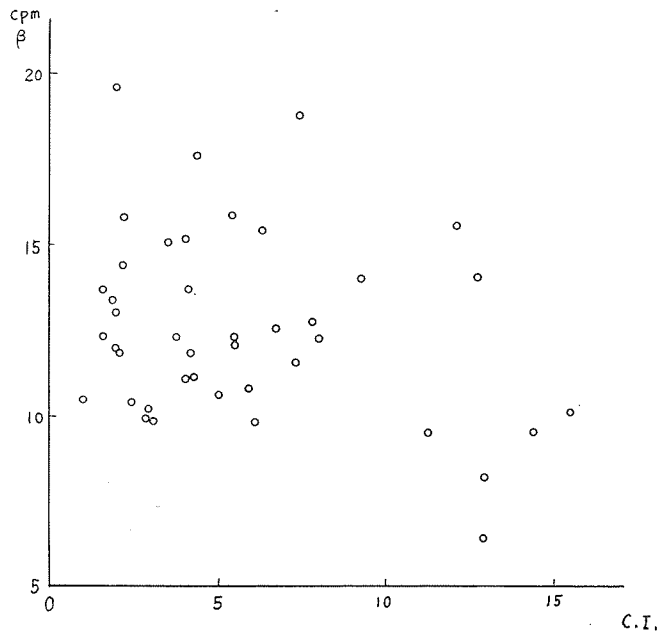

Fig. 7-2. Relationship between beta-radioactivity and colour index.

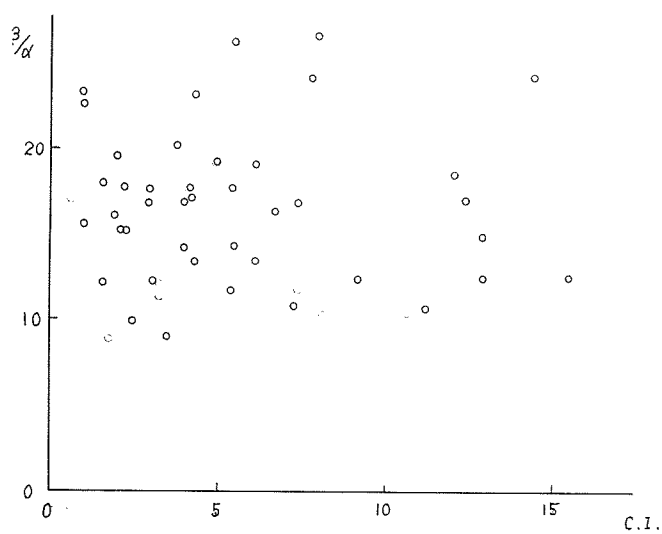

Fig. 7-3. Relationship between β/α ratio and colour index.

apparently unrelated to colour index, but β/α ratio increase with increasing colour index.

The relationships between alpha- and beta-radioactivities and β/α ratio, and quartz content are shown in Figs. 8-1 to 8-3. Plots of β/α ratio vs. quartz content shows no correlation.

β/α ratio increases with increasing potash-feldspar, as shown in Fig. 9, but the relationship between radioactivity and potash-feldspar content is obscure.

Table 9 shows the alpha-radioactivity and beta-radioactivity increase with an decrease in anorthite content of plagioclase.

In summary, mineral contents by modal analyses are very vague but appear to have a rough relationship to the radioactivity and type of granite. The difference of points in the diagram is caused partly by within-pluton variation and partly by sampling variation. Much of the scatter may be caused by general imperfection of petrogenetic control of the uranium and thorium. From this study of the granitic rocks representing different environments and different types of genesis, the granite intrusion may contain different amounts of thorium and uranium even though their major components may be equal, and these differences may cause a significant amount of variation.

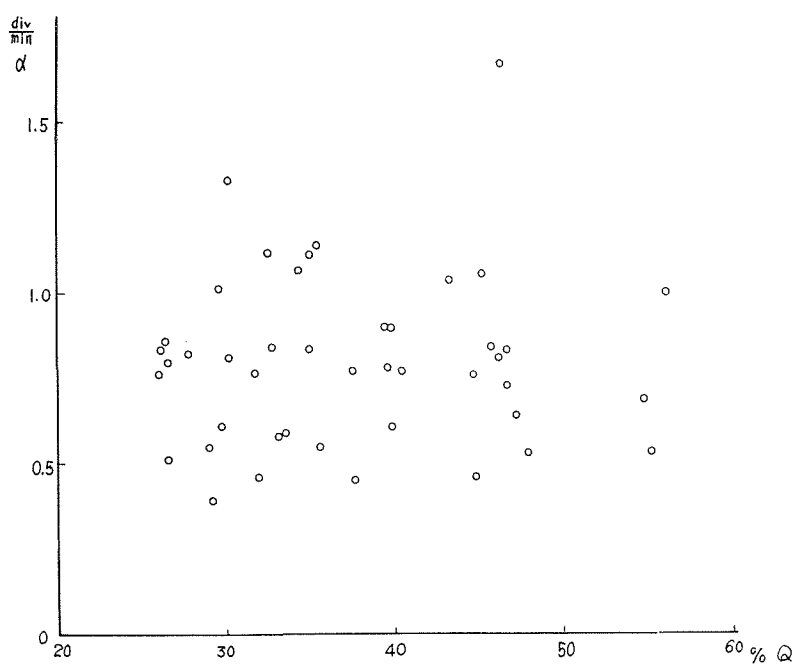

Fig. 8-1. Relationship between alpha-radioactivity and quartz content.

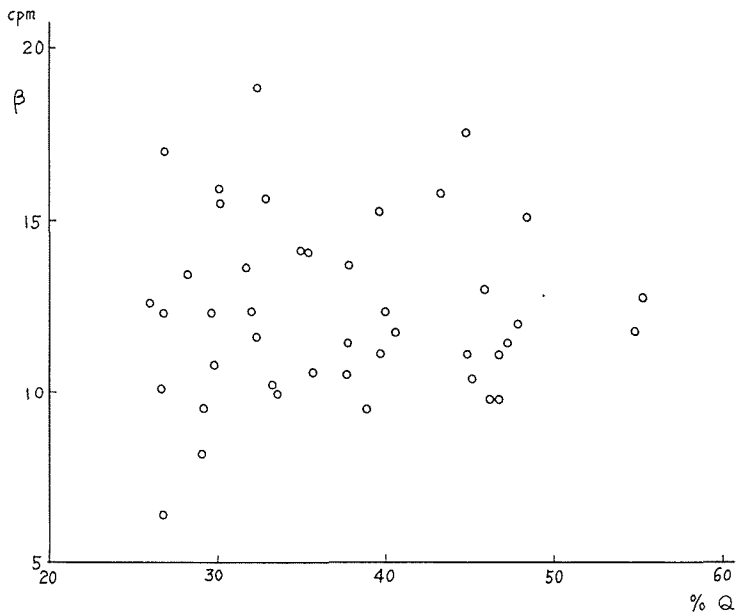

Fig. 8-2. Relationship between beta-radioactivity and quartz content.

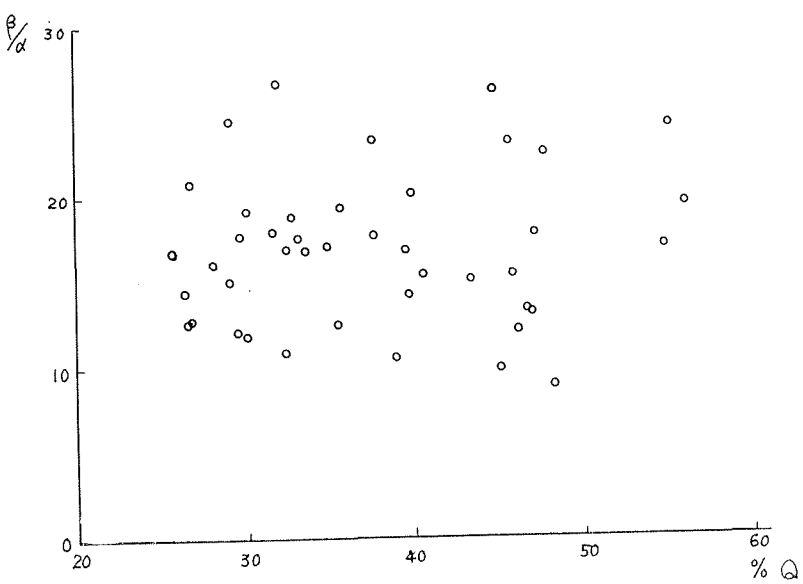

Fig. 8-3. Relationship between β/α ratio and quartz content.

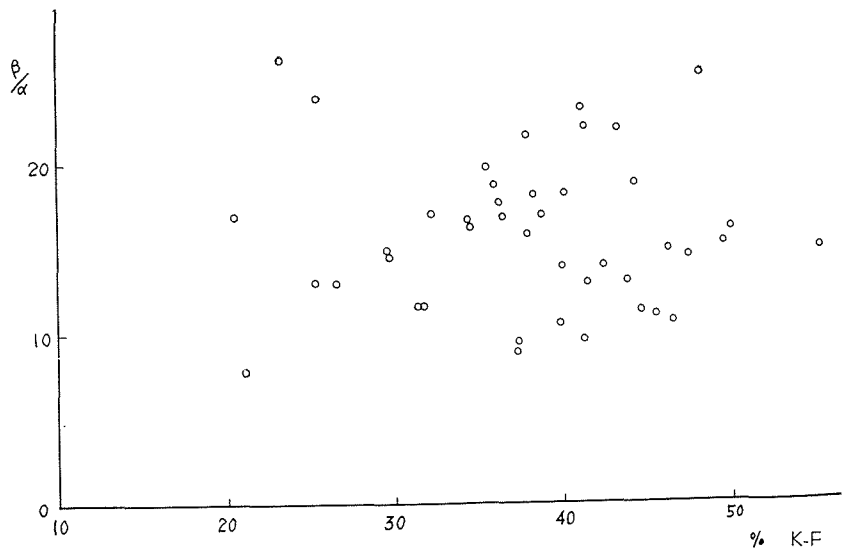

Fig. 9. Scatter diagram β/α ratio vs. potash-feldspar.

Conclusions

(1) The content differences of minerals of various different types of granitic rocks are smaller than those within individual intrusions.
(2) In view of mineral assemblage and radioactivity, the Kitashirakawa granitic mass may be divided into two parts.
(2) Beta-radioactivity and β/α ratio increase slightly with increasing R.
(4) β/α ratio increases with increasing colour index.
(5) The relationship between radioactivity and quartz content indicates a slight increase in radioactivity with increasing quartz content.
(6) Radioactivity increases at an increasing rate with decrease in anorthite content of plagioclase.

Acknowledgment

The writer is greatly indebted to the kind guidance by Prof. Z. Hatuda throughout the present study, and also he wishes to express his sincere thanks to Dr. K. Morita and Dr. S. Enomoto of the Nagoya Technical Industrial Laboratory for their generous permission of using their valuable apparatus in spectrographic analyses and beta-radioactivity measurement. Further, the writer wishes to thank Prof. T. Asayama of the Osaka Prefectural University for quoting his data on radium content of granites in Kitashirakawa and

Tanakami-Mikumo areas. The sampling work reported in this paper was done largely supported by Mr. K. Katsura, and this manuscript was corrected by Dr. R. W. Girdler of the University of Durham, the writer wishes to express his thanks to them for their kindness. Lastly, this investigation has been partly supported by the financial aid of the Scientific Research Expenditure of the Ministry of Education.

Literature

1) INGHAM, W. N. and N. B. KEEVIL; Bull. Geol. Soc. Amer., **62**, pp. 131–148, (1951).
2) HATUDA, Z. and I. YUN: Rep. Balne. Lab., Okayama Univ., **19**, pp. 9–15, (1957).
3) HAMILTON, E.: Medd. on Gφnland., Bd. **162**, 8, pp. 1–41, (1961).
4) NISHIMURA, S.: Mem. Coll. Sci., Kyoto Univ., **B**, **28**, pp. 265–284, (1961).
5) ADAMS, J.A.S., J. K. OSMOND and J. J. W. ROGERS; Phys. Chem. Earth **3**, pp. 398–348, (1959).
6) HATUDA, Z. and J. NAGAI; Mem. Coll. Sci., Kyoto Univ., **B**, **28**, pp. 527–538, (1962).
7) FINNEY, G. D. and R. D. EVANS; Phys. Rev., **48**, pp. 503–511, (1935).
8) HATUDA, Z. and S. NISHIMURA; Mem. Coll. Sci., Kyoto Univ. **B**, **23**, pp. 285–295, (1956).
9) ASAYAMA, T.; Jour. Astro. Geophys., **16**, pp. 9–26, (1936).
10) ASAYAMA, T.; Mem. Indi. Arts., Kyoto Tech. Univ., Sci. Tech., **3**, **b**, pp. 25–54, (1954).
11) UEJI, T.: Jour. Geography, **49**, pp. 481–497, (1937).
12) WHITEFIELD, J. M., J. J. W. ROGERS and J. A. S. ADAMS; Geochim. Cosmochim. Acta, **17**, pp. 248–271, (1959).